



International Conference on Concentrating Solar Power and Chemical Energy Systems,  
SolarPACES 2014

## Investigation of heat loss from a solar cavity receiver

E. Abbasi-Shavazi<sup>a,\*</sup>, G.O. Hughes<sup>b</sup>, J.D. Pye<sup>a</sup>

<sup>a</sup> Solar Thermal Group, Research School of Engineering, The Australian National University, Canberra, ACT 0200 Australia

<sup>b</sup> Research School of Earth Sciences, The Australian National University, Canberra, ACT 0200 Australia

---

### Abstract

This study examines experimentally the heat loss from a model solar cavity receiver. For this purpose, laboratory-scale cylindrical cavity models with geometric aspect ratios (cavity length to diameter) of 1 and 2, and aperture opening ratios (aperture diameter to cavity diameter) of 0.5 and 1, were built. Each cavity was subjected to constant boundary heat input via heating cables, and was operated at various downward inclinations. A carefully-applied coating of Pyromark-2500 heat resistant paint on the cavity surface, in conjunction with steady-state experimental temperatures, enabled accurate calculation of the radiative loss from the cavities. The experimental technique allowed precise control of the operating parameters, resulting in determination of the conduction loss, and subsequently, the convection heat loss. Operation at temperatures up to 650°C allowed for a better understanding of the interaction between radiation and convection heat loss mechanisms.

Experimental data obtained in this study are shown to be consistent with the concept of stagnation and convection zone development in cavities, with increasing cavity inclination angle. A qualitative assessment of the impact of these zones on the cavity surface temperatures is presented. Whereas thermocouples located in stagnation region show uniform temperature distribution, the surfaces which are exposed to convective flows exhibit larger temperature variations. The temperature distribution along the cavity walls and its effect on radiative loss calculation is also investigated in this work. It is seen that radiative loss predictions which consider an average cavity temperature in their model can overestimate the losses due to this mechanism by up to 20%, in comparison to models which use experimental temperatures along the cavity interior. Convection loss from the cavity is calculated and compared with results from correlations proposed in the literature. It is seen that correlations based on surface areas of the stagnation and convection zones are better at predicting the experimental results.

© 2015 The Authors. Published by Elsevier Ltd.

Peer review by the scientific conference committee of SolarPACES 2014 under responsibility of PSE AG.

*Keywords:* Experimental heat transfer; Convection heat loss; Receiver design

---

\* Corresponding author. Tel.: +61-2-6125 0411

E-mail address: [ehsan.abbasi@anu.edu.au](mailto:ehsan.abbasi@anu.edu.au)

**Nomenclature**

$AR$	Aspect ratio, defined as cavity length to diameter
$D$	Cavity diameter
$L$	Cavity length
$OR$	Aperture opening ratio, defined as aperture diameter to cavity diameter
$P_{in}$	Electrical power input into heating coil
$Q_{conv}$	Convection heat transfer rate
$Q_{cond}$	Conduction heat transfer rate
$Q_{Rad}$	Radiation heat transfer rate
$\theta$	Cavity inclination angle, as measured from horizontal. Downward direction is positive.

**1. Introduction**

Technologies and methods to utilize concentrated solar energy have been the subject of research and development for a number of decades. Recently, a concerted effort is being made to achieve higher operating temperatures and efficiencies in solar thermal systems, allowing concentrating solar power (CSP) to become more affordable in comparison to fossil-fuel generated electricity [1,2].

Concentrating solar dish technology is one of the configurations used in CSP plants. Cavity-shaped receivers are positioned at the focus of the dish, allowing for collection of concentrated solar irradiation. A schematic diagram of a concentrating solar dish is shown in Fig. 1. In comparison to volumetric receivers, cavity receivers are expected to have reduced convection and radiation heat loss to the environment due to their lower view factor to the surroundings. Nevertheless, the high temperatures resulting from concentrations of up to 1500 suns in dish systems can serve to increase thermal losses from these systems if adequate heat loss suppression practices are not employed. Accurate knowledge of heat transfer in solar receivers is thus necessary to allow better cavity designs and to increase the operating efficiencies and cost effectiveness of CSP systems. It is widely acknowledged that of the conduction, radiation and convection losses from solar cavity receivers, determination of latter is the most complex [3,4]. This is due to the numerous parameters that affect convective heat loss, which include the large size, varying incident flux, and complex geometries of the receivers. Environmental operating conditions such as wind velocity and direction also have a significant impact on these convective losses because the cavity receivers are open to the surroundings. Nevertheless, through systematic analysis of experimental data and numerical modelling, the resulting observations, insights and quantitative findings are important in better understanding convective heat loss from solar cavities.

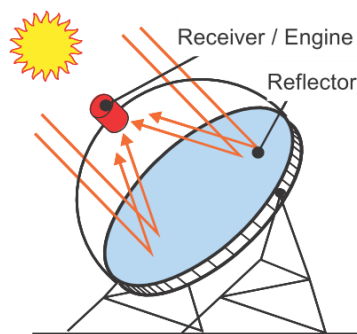


Fig. 1 Schematic diagram of a concentrating solar dish system. Obtained from [5]

Initial research on this topic focused on cubical cavity receivers. Eyler [6] used a two-dimensional finite-difference CFD code to model the natural convection from two sample cavities. His results confirmed the dependency of convective loss on cavity dimensions and wall temperature. Le Quere et al [7] undertook numerical

and experimental investigations of convective loss in two cubical cavities, with dimensions of  $0.2\text{m} \times 0.2\text{m} \times 0.2\text{m}$  and  $0.6\text{m} \times 0.6\text{m} \times 0.6\text{m}$ . The sidewalls of the cavities studied in their work were made of borosilicate glass plates, allowing for optical investigation of convective flows in the cavity, which was operated at both positive (i.e. downward) and negative (upward) inclinations. Clausing [3] was the first to propose an analytical model that took into consideration the presence of two distinct regions within cavities, namely a stagnation zone and a convective zone. He hypothesised that convective heat loss depended on two main factors; 1) the ability to transfer mass and energy across the aperture, and 2) the ability to heat the air inside the cavity. Subsequent work by Clausing [8] used experimental data to provide more accurate correlations. Further experimental work by Siebers and Kraabel [9] and Leibfried and Ortjahan [10] incorporated the effect of parameters measuring the ratio of wall-to-ambient temperature, as well as various length definitions to model stagnation and convection zones in cubical cavity receivers.

With dish collector applications in mind, studies have been conducted on cylindrical and hemispherical cavities. Koenig & Marvin, as reported in Harris and Lenz [4], conducted an experimental study on natural convection loss from a cylindrical cavity receiver, subjected to on-sun conditions. McDonald [11] used a cylindrical-frustum shaped cavity in controlled laboratory experiments to obtain the convective heat loss. The cavity was heated using a hot heat transfer fluid, and the heat losses were determined from thermocouple readings at various locations in the cavity, including the inlet and outlet fluid temperatures. Bulk cavity operating temperatures were between  $149^\circ\text{C}$  and  $316^\circ\text{C}$ . Extensive work has been undertaken at The Australian National University [12-15] on experimental and numerical modelling of cylindrical cavity receivers because of a historical research emphasis on paraboloidal dish systems. Paitoonsurikarn et al [14] reported a correlation based on numerical modelling of four different cavity geometries, and comparison of the results with two sets of experimental data. The proposed correlation included an “ensemble cavity length” in the Nusselt number definition which aims to model the effect of inclination and the development of stagnation and convective zones in a cavity by defining different length parameters. Taumoeolau et al [15] reported experimental results from an electrically heated cavity. Results from his work showed that for a cavity oriented vertically-downward, the convective heat loss was not equal to zero. The correlation derived from this study was thus in contrast to previous work in the literature. Subsequent experiments have confirmed this finding [16]. Recently, Wu et al [17] and Wu et al [18] have reported results from electrically heated cylindrical cavity models, testing the effect of constant heat flux and rotation of the cavity, respectively, on convective losses.

This study examines experimentally the convective loss from a model cylindrical solar cavity receiver, as a function of applied heat input, cavity temperature and inclination angle. The investigation has also explored the effect on convective losses of the cavity aspect ratio and aperture opening ratio, however, these data are the focus of further investigation and will not be reported on here. The aim of this paper is to provide experimental data for inclusion in the literature on this topic, to compare results with the previous work in this field, and to also gain a better understanding of the interplay between radiative and convective heat transfer mechanisms in a cavity receiver. The experimental data in this study are also benchmarked against the predictions of a number of correlations proposed in the literature, sources of discrepancy are commented upon, and suggestions are made for development of improved correlations by examining aspects of convective loss not yet considered.

## 2. Experimental setup and procedure

An electrically-heated cavity receiver model was constructed based on a design studied previously at The Australian National University [15]. The experimental heat loss data obtained from the laboratory setup was designed to enable comparison of the results with those cited in the literature. The following sections describe the experimental setup, experimental procedure and data reduction methods.

### 2.1. Experimental setup

The experimental setup and a cross-section of the cavity receiver used in this study are shown in Figs. 2 and 3. As can be seen in Fig. 2, the model receiver is attached to a stepper motor, using two L-shaped hinges. The stepper motor mechanism allows the cavity to be inclined at various angles during the experiment. A Eurotherm power controller is used to deliver constant power to the heating cable. Thermocouple data is acquired at a frequency of

2Hz using a National Instruments 9213 data logger. A LabView program is used to operate the Eurotherm power controller, record temperature data from thermocouples, and also alter cavity inclination angle for each experiment. An NEC H2640 infrared thermal imaging camera was also used to visually inspect the cavity wall temperature profile.

The model receiver consists of a stainless steel-316 cylindrical cavity, with an internal diameter  $D$  of 83mm and a wall thickness of 3mm. Two different cavities with lengths  $L$  of 83mm and 166mm are used to obtain data sets for cavities with aspect ratio  $AR$  ( $=L/D$ ) of 1 and 2. A Magnesium oxide-insulated, stainless steel-sheathed heating cable, having a Nichrome conductor, is tightly wound and fastened to the outer surface of the cylinder to ensure good thermal contact. The inner surface of the cylindrical cavity is first sand-blasted, to provide a smooth finish, and then coated with Pyromark-2500 flat-black solar-grade heat resistant paint. To obtain the ideal thermal properties from the paint, as well as perfect adhesion of the paint to the surface, curing is performed by heating the cavity to 250°C for two hours and then allowing the surface to air dry for 18 hours. To ensure that a minimum amount of heat is lost due to conduction, two types of insulation are used. Two circular Superwool Plus insulation boards are attached to the back (unheated) wall of the cavity, as shown in Fig. 3a. The remaining volume between the cavity and receiver casing is filled with layers of Isowool ceramic fiber blanket insulation.

To obtain temperature values at various positions along the cavity wall, thermocouples are embedded in the cavity wall. More specifically, holes are drilled into the cavity outer surface, terminating 1mm from the inner wall. Thermocouples are then braised into the surface at the location of these holes. A total of 13 K-type thermocouples are used in the experiments. For both cylindrical cavities, 11 thermocouples measure the cavity side- and back-wall temperatures, and two thermocouples measure the side and back wall temperature of the receiver casing. Fig. 3b shows representative location of the thermocouples for the cavity of  $AR=2$ .

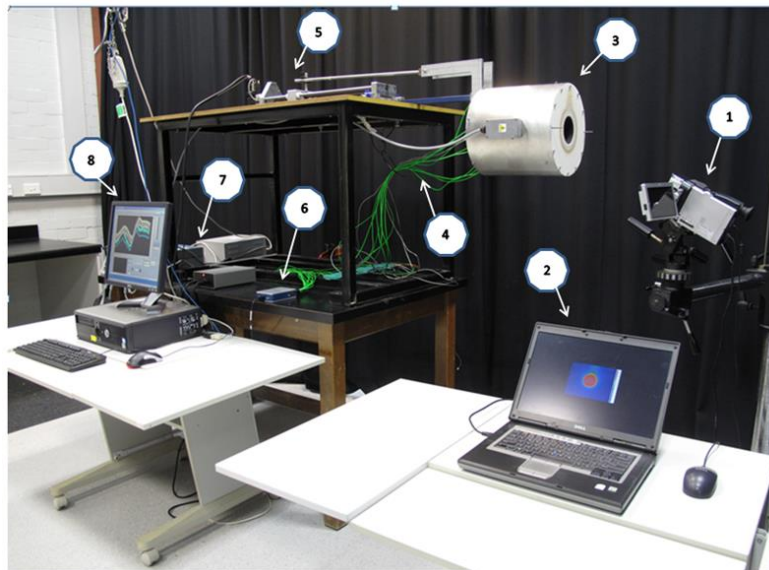


Fig. 2. Experimental setup for natural convection experiments – 1: Thermal camera, 2: Laptop, for thermal image acquisition, 3: Model cavity receiver, 4: Thermocouple connections, 5: Stepper motor, 6: Data logger, 7: Power controller, 8: PC used for data acquisition.

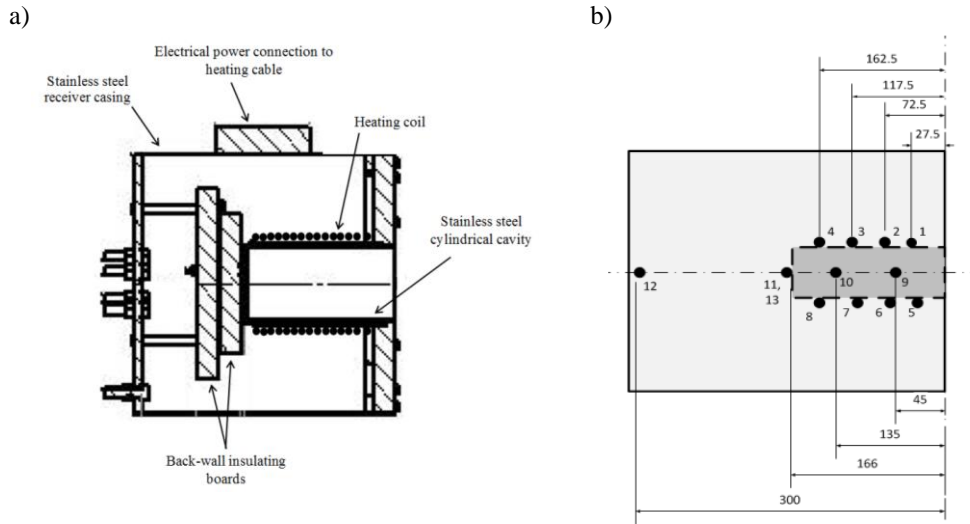


Fig. 3 Cross section sketch of lab-scale cavity receiver, showing a) different components of the receiver, b) thermocouple locations for cavity with  $AR=2$

### 2.2. Determination of energy balance

During each experiment, the total losses in the system are maintained at a constant value (equal to the power input to the heating cable). Once the system operates at steady state, the power delivered to the heating cable is lost by conduction, convection and radiation to the surroundings, as represented in Eq. 1,

$$P_{in} = Q_{cond} + Q_{conv} + Q_{rad} \quad (1)$$

Here  $P_{in}$  is the value set in the Eurotherm power controller, and the convective loss  $Q_{conv}$  must be indirectly evaluated based on knowledge of  $Q_{cond}$  and  $Q_{Rad}$ .

### 2.3. Experimental procedure

The total input power to the heating cable that was needed to deliver maximum local temperatures in the cavity of  $450^{\circ}\text{C}$ ,  $550^{\circ}\text{C}$  and  $650^{\circ}\text{C}$  was first determined. During an experiment the cavity was initially positioned at a downward inclination, corresponding to  $90^{\circ}$  from the horizontal. The setup was heated with the chosen constant power level until steady-state was reached. The definition of steady-state used in the experiments was a change in temperature recorded by each thermocouple of less than  $1^{\circ}\text{C}/\text{hour}$ . Steady-state temperatures were obtained by following this procedure for inclination angles between  $90^{\circ}$  and  $0^{\circ}$  (horizontal), in  $15^{\circ}$  increments, for cavities of  $AR=1$  and  $AR=2$ . A number of experiments were repeated over the space of a number of weeks to assess repeatability. It was found that steady-state temperatures were reproducible with great consistency.

### 2.4. Conduction loss experiments

The conduction loss at each cavity inclination was obtained by suppressing convection and radiation losses from the aperture. A solid circular plug with low thermal conductivity was positioned at the aperture, and kept tightly in place. Given that temperatures in the cavity changed with each inclination during the natural convection experiments, the corresponding average cavity temperature was recreated during each conduction loss experiment. For this purpose, average cavity temperatures during natural convection experiments were calculated, and input

power to the heating cable was varied until a steady-state temperature equivalent to the temperature was obtained. The value of input power was thus determined to be the conduction heat loss through the side and back wall of the receiver, and also through the plug. The heat loss from the plug was obtained by using a conduction thermal resistance model, coupled with estimates of temperatures on the internal and external surfaces of the plug. It should be noted that while other experimental studies in the literature have calculated conduction losses using only a one-dimensional thermal resistance network [17], the current study combines experimental temperature data with a resistance network model to capture realistic effects, such as air gaps that might be present due to insulation placement around the cavity, as alluded to by Wu et al [18].

### 2.5. Radiation loss calculation

Calculation of radiation heat loss was undertaken using a radiosity network model utilizing axisymmetric assumptions. The temperature values used in the radiosity network method were obtained from experimental data. Given that the cavity surface was coated with a carefully-applied layer of Pyromark-2500 paint, the total hemispherical emissivity was assumed to be between 0.87-0.89, based on data obtained for Pyromark-2500 on cold-rolled steel at 600°C [19]. As part of the data analysis, various definitions of representative cavity temperatures were implemented for the radiation loss modelling. This is discussed in detail in Section 3.2

## 3. Results and discussion

### 3.1. Cavity temperature profile

Figs. 4a and 4b show the temperature distribution along the top and bottom surface of the cavity with  $AR=2$ . The total power input into the cavity is 200 W, which equates to  $4260\text{W/m}^2$ . The data points represent thermocouple readings at the specified locations. For a constant heat input, all thermocouples show an increase in temperature as the inclination angle increases from  $\theta=0^\circ$  to  $\theta=90^\circ$ . This behavior is consistent with the concept of stagnation and convection zones. At horizontal inclination, the incoming stream of ambient air experiences a decrease in density as it flows along the hot bottom wall. This results in the air rising towards the top surface, and leaving from the top of the aperture. At an angle of  $\theta=30^\circ$ , a stagnation zone forms along the top surface of the cavity. The reduced displacement of this volume of air allows the temperature in this region to rise, which is consistent with the uniform increase in each of the thermocouple readings in Fig. 4a as inclination angle increases. Fig. 4b further supports this argument. As cavity angle increases from  $\theta=0^\circ$  to  $\theta=30^\circ$ , only the thermocouple located at  $z/L=0.94$  is situated in the stagnation zone, and shows the largest relative increase in temperature. Other thermocouples are in the convective zone, and the flow entering the cavity serves to limit the increase in temperature of these thermocouples. The trend line for  $\theta=60^\circ$  shows the thermocouple located close to the aperture is greatly influenced by the convective flow leaving the cavity. At  $\theta=90^\circ$ , this thermocouple becomes fully situated in the stagnation zone and shows the largest relative increase in temperature. Comparison of Figs. 4a and 4b at  $\theta=90^\circ$  indicates an axially uniform temperature distribution is established in the cavity.

While the convective flows into and out of the cavity influence the temperature distribution along the wall, significant and systematic spatial variations are associated with the local view factors of each region to the aperture. The region closest to the cavity aperture has the largest view factor and hence the largest local radiative loss (for a given total heat input). As this view factor effect alone would result in an axially symmetric temperature distribution, an indication of the importance of convective losses can be made by examining the departure from axial symmetry in Figs. 4a and 4b. It is apparent in Fig. 4b that the ambient air entering the bottom of the cavity further reduces the lower wall temperatures, especially in the region close to the aperture. It might be expected that the thermocouple located at  $z/L=0.94$  would show a higher temperature than the thermocouple at  $z/L=0.67$ . One possibility for this trend not being seen in the results could be due to conduction heat loss to the unheated back-wall which is adjacent to this thermocouple.

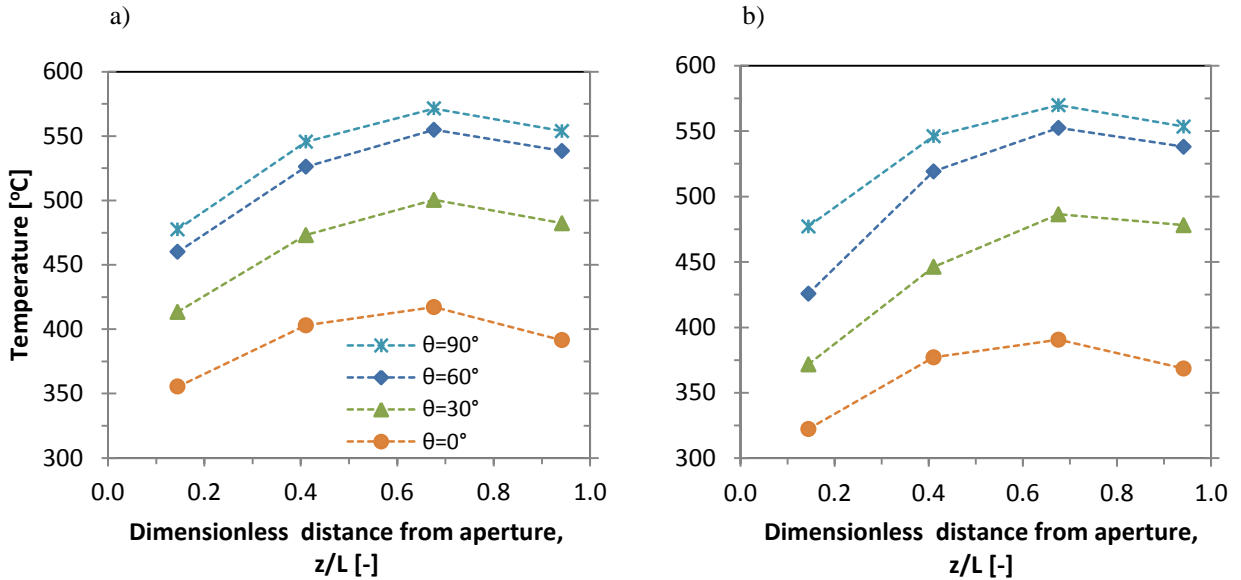


Fig. 4 Surface temperature distribution inside the cavity with AR=2,  $q=4260\text{W/m}^2$ : a) top surface. b) bottom surface. The legend in Fig. 4a can also be used for Fig. 4b

### 3.2. Influence of temperature variation on radiation loss calculation

Given the temperature distribution which exists in the cavity, it is important that a reasonable assumption is made regarding the representative temperature of the cavity when undertaking radiation loss calculations. It would seem that a radiative heat loss model which accounts for the non-axisymmetric temperature profile in the cavity would provide the most accurate result. The study by Wu et al [18], in which an electrically heated cylindrical cavity is used to investigate the effect of cavity rotation on convection loss, uses this approach. The work by Wu et al [17], which studies convective heat loss in a cylindrical cavity subjected to constant heat flux, undertakes a simpler calculation of radiative loss based on a single temperature. Figure 5 compares values of radiative loss obtained using different assumptions for the cavity temperature. The radiative loss based on the area-weighted average temperature is obtained by taking the average value of all thermocouple values on the top and bottom surface of the cavity. This approach is frequently used in the experimental heat loss studies, and can be seen to lead to a relatively high estimate of the radiation loss. This occurs because all regions in the cavity are assumed to be at a constant temperature (including regions close to the aperture as well as the regions towards to back of the cavity) and the loss varies with the fourth power of the average temperature. In using the top or bottom surface temperatures to calculate the loss, an axially symmetric temperature distribution is assumed that corresponds to a curve fit of the top or bottom temperature profile measured along the cavity. This curve is used in conjunction with a program that uses the radiosity network method to calculate and sum the local radiation losses. Given that the top surface has higher temperatures, the radiative loss estimate is seen to lie above that based on the bottom surface temperatures. Importantly, comparison of radiation loss values based on bottom surface and area-weighted cavity average temperature shows no more than a 10-20% difference. The largest discrepancy between these values occurs at  $45^\circ$  cavity inclination. This means that temperature variation is a critical factor to take into consideration when modelling solar cavity receivers.

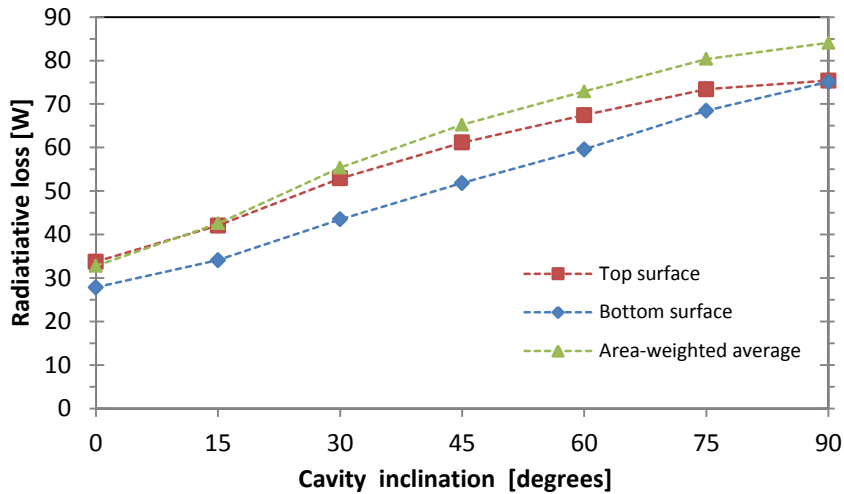


Fig. 5 Comparison of radiative loss values based on difference cavity temperature assumptions

### 3.3. Comparison of convection loss results to literature

Using the method outlined in Section 2.2, the convection heat loss is obtained for each experiment. A representative plot is presented, in Fig. 6, corresponding to the experiments for a cavity with  $AR=2$ ,  $P_{in}=150$  W. The error bars are based on the calculations for the different assumptions discussed in Section 3.2 regarding the temperature profile. The top wall temperatures are used to calculate the radiation loss. Error values correspond to the difference observed for each data point at inclination angles shown in Fig. 5. For the case in Fig. 6, it is seen that the Stine [20] and Koenig [4] correlations overestimate the losses for inclinations less than  $45^\circ$ , and underestimate the losses for higher tilt angles ( $\theta > 45^\circ$ ). These two correlations also estimate convective losses at an angle of  $15^\circ$  that are higher than the horizontal case. This is due to the fact that the average cavity temperature at  $\theta=15^\circ$  is much higher than that for a horizontal cavity. It is interesting to note that all the other correlations, except Wu et al [17], estimate decreasing convection loss as cavity inclination increases. The reason is that these correlations take some account of the formation of convection and stagnation zones. The Jilte et al [21] correlation explicitly uses cavity wall area below the stagnation zone in addition to the horizontal area separating the stagnation and convection regions in calculating convection loss. The modified Stine [10] and Taumofolau [22] correlations used area ratios in the calculation of Nusselt numbers, resulting in the decreasing trend. The correlation by Paitoonsurikarn et al [14] underestimates the losses to for all angles, despite having been formulated based on cylindrical cavities. This systematic underestimation has also been noted by Wu et al [18]. The geometry and experimental method used in this study fulfils all the criteria stated for the correlation proposed by Wu et al [17], but as seen in Fig. 6, the result is not satisfactory. The authors suggest that more detailed assumptions are likely required in modelling the conduction and radiation losses, and hence formulating the convective loss correlation. More specifically, the conduction model used should take into account experimental results in addition to resistance network modelling. Nevertheless, the results from the current study can be used to further improve this correlation. One suggestion is the inclusion of a representative wall temperature in the formulation of the Nusselt number. As it stands, the correlation only uses the ambient temperature to evaluate fluid properties. Whereas in other correlations, a ratio of wall-to-ambient temperature is used in the Nusselt number correlation, the correlation suggested by Wu et al [17] uses a “bulk temperature” which is arbitrarily assigned as 298K. No justification has been made by the authors as to the origin of this temperature, and the purpose which the ratio of ambient-to-bulk temperature serves, given that in most cases it is equal to a value of one.

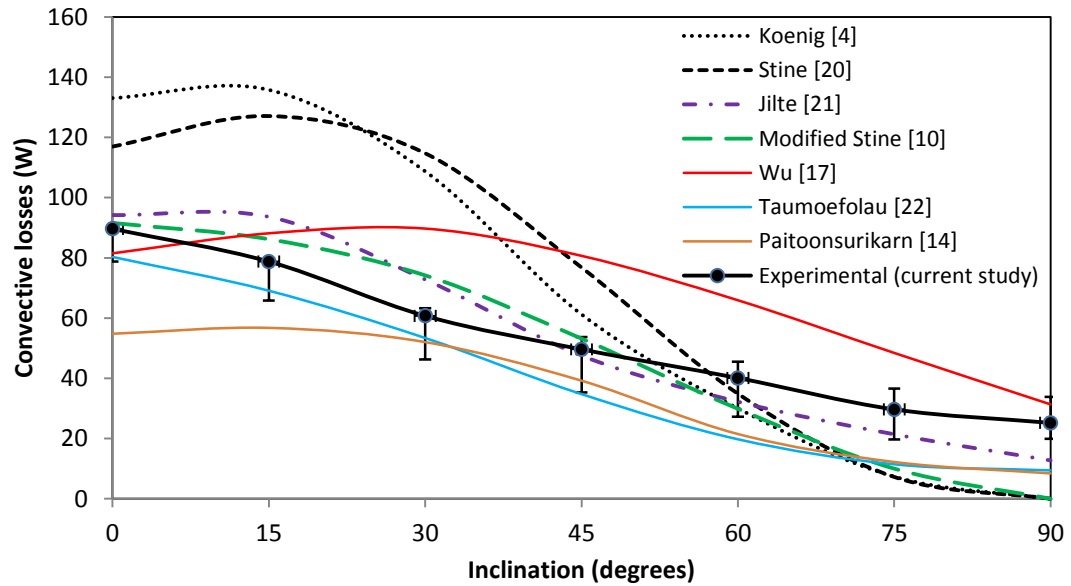


Fig. 6 Comparison of experimental data from current study to correlations cited in literature

The current study also undertook experiments for a cavity with  $AR=1$  and further obtained data for both the  $AR = 1$  and  $2$  cavities with constrained apertures. Further analysis of the data is currently underway and is not presented here.

#### 4. Conclusion

Experimental data serve as invaluable tools in modelling heat loss from cavity receivers, and are important to complement the numerical investigations undertaken on this topic. The current work has studied the convective heat loss from a cylindrical cavity receiver, subject to a range of constant heat input boundary conditions. The temperature distribution along the cavity walls is seen to vary naturally because of local radiative and convective heat transfer, and is a function of cavity inclination. The experimental data has been used to obtain upper and lower bounds for the components of overall convective and radiative heat loss. The large and systematic temperature variations observed in the model cavity studied here lead us to conclude that it is questionable whether constant wall temperature assumptions used cavity convective heat loss correlations are sufficiently accurate for predictive purposes. As such, further investigations on the role of cavity temperature variation in predicting convective losses form part of ongoing work.

#### Acknowledgements

Funding for this work was provided by the Australian Renewable Energy Agency. GH was supported by Australian Research Council Future Fellowship FT100100869. The authors wish to thank T. Beasley and B. Tranter from the Geophysical Fluid Dynamics Laboratory at The Australian National University for assistance with the experimental setup. Provision of a thermal imaging camera from CSIRO Energy Centre is also gratefully acknowledged.

#### References

[1] Australian Solar Thermal Research Initiative, 2014. Available online at: <http://www.astr.org.au/>

- [2] NREL, 2012. Sunshot Vision Study. National Renewable Energy Laboratory, Report No: DOE/GO-102012-3037
- [3] Clausing, A. M. 1981. An analysis of convective losses from cavity solar central receivers. *Solar Energy*, **27**, 295-300.
- [4] Harris, J. A. & Lenz, T. G. 1985. Thermal performance of solar concentrator/cavity receiver systems. *Solar Energy*, **34**, 135-142.
- [5] Romero, M., Gonzalez-Aguilar, J., 2014. Solar thermal CSP technology *WIREs Energy Environ*, **3**, 42–59
- [6] Eyler, L.L., (1980), Predictions of convective losses from a solar cavity receiver, Proceedings for the Century 2 Solar Energy Conference, San Francisco, California
- [7] Le Quere, P., Penot, F. & Mirenayat, M. 1981. Experimental study of heat loss through natural convection from an isothermal cubic open cavity, Sandia National Laboratories, SAND81-8014
- [8] Clausing, A. M., Waldvogel, J. M. & Lister, L. D. 1987. Natural convection from isothermal cubical cavities with a variety of side-facing apertures. *Journal of Heat Transfer*, **109**, 407-412.
- [9] Siebers, D.L. & Kraabel, J. S., 1984. Estimating convective energy losses from solar central receivers, Sandia National Laboratories, USA
- [10] Leibfried, U. & Ortjohann, J. 1995. Convective heat loss from upward and downward-facing cavity solar receivers: measurements and calculations. *Journal of Solar Energy Engineering*, **117**, 75-84.
- [11] McDonlad, C. G. 1995. Heat loss from an open cavity. Sandia National Laboratories, SAND95-2939
- [12] Paitoonsurikarn, S., Taumoefolau, T., & Lovegrove, K. 2004. Estimation of convection loss from paraboloidal dish cavity receivers. *Solar 2004: Life, the universe and renewables*. Perth, Australia.
- [13] Yeh, K. C., Hughes, G. & Lovegrove, K. 2005. Modelling the convective flow in solar thermal receivers. *43rd Conference of the Australia and New Zealand Solar Energy Society (ANZES)*. Dunedin, New Zealand.
- [14] Paitoonsurikarn, S., Lovegrove, K. Hughes, G. & Pye, J. 2011. Numerical investigation of natural convection loss from cavity receivers in solar dish applications. *Journal of Solar Energy Engineering*, **133**, 021004-1-021004-10.
- [15] Taumoefolau, T., Paitoonsurikarn, S., Hughes, G. & Lovegrove, K. 2004. Experimental investigation of natural convection heat loss from a model solar concentrator cavity receiver. *Journal of Solar Energy Engineering*, **126**, 801-807.
- [16] Prakash, M., Kedare, S. B. & Nayak, J. K. 2009. Investigations on heat losses from a solar cavity receiver. *Solar Energy*, **83**, 157-170.
- [17] Wu, S.-Y., Guan, J.-Y., Xiao, L., Shen, Z.-G. & Xu, L.-H. 2013. Experimental investigation on heat loss of a fully open cylindrical cavity with different boundary conditions. *Experimental Thermal and Fluid Science*, **45**, 92-101.
- [18] Wu, W., Amsbeck, L., Buck, R., Waibel, N., Langner, P., Pitz-Paal, R., 2014. On the influence of rotation on thermal convection in a rotating cavity for solar receiver applications. *Applied Thermal Engineering* **70** (1) pp. 694-704
- [19] Ho, C. K., Mahoney, A. R., Amborsini, A., Bencomo, M., Hall, A. & Lambert, T. N. 2012. Characterization of Pyromark 2500 for high-temperature solar receivers. *6th International Conference on Energy Sustainability and 10th Fuel Cell Science, Engineering and Technology Conference (ESFuelCell2012)*. San Diego, USA.
- [20] Stine, W. B. & McDonald, C. G. 1989. Cavity receiver convective heat loss. *Congress of the ISES*. Kobe, Japan.
- [21] R. D. Jilte, S. B. Kedare, J. K. Nayak, 2013. Natural convection and radiation heat loss from open cavities of different shapes and sizes used with dish concentrator, *Mechanical Engineering Research*, **3**, 25-43.
- [22] Taumoefolau, T. I. 2004. *Experimental investigation of convection loss from a model solar concentrator cavity receiver*. M.Phil thesis, The Australian National University.